CERN LIBRARIES, GENEVA

CERN/SPSC/ 78-54
SPSC/ P93-Add.1

May 10th 1978

ADDENDUM TO THE PROPOSAL

TO STUDY ANTIPROTON-PROTON INTERACTIONS

AT 540 GEV CM ENERGY

***

M. Banner [1], H-J. Besch [2], L. Camilleri [2], J.C. Chollet [3],
A.G. Clark [2], C. Conta [4], P. Darriulat [2], L. Di Lella [2],
M. Fraternali [4], D. Froidevaux [3], J-M. Gaillard [3], G. Goggi* [4],
V. Hungerbühler [2], F. Impellizzeri [4], M. Livan [4], G.C. Mantovani [4],
B. Merkel [3], F. Pastore [4], P. Perez [1], H. Plothow* [3],
S.H. Pordes [2], J-P. Repellin [3], G. Sauvage [3], G. Smadja [1],
J. Teiger [1], C. Tur [1], H. Zaccone [1], and A. Zylberstejn [1].

CERN - ORSAY - PAVIA - SACLAY COLLABORATION

[1] CEN-Saclay, France
[2] CERN, Geneva, Switzerland
[3] LAL-Orsay, France
[4] University of Pavia and INFN, Sezione di Pavia, Italy

 * Presently CERN, Geneva, Switzerland

INTRODUCTION

Following a request from the Chairman of the SPSC we are providing the Committee with some additional information concerning our proposed experiment (P93).

We present this information in five different sections :

1 - GENERAL COMMENTS ON THE PROPOSED DESIGN.

2 - BACKGROUNDS IN THE SEARCH FOR W → eν.

3 - THE FORWARD AND BACKWARD DETECTORS.

4 - DETECTOR DESIGN : MECHANICAL ASPECTS.

5 - MEMBERSHIP OF THE COLLABORATION.

1 - GENERAL COMMENTS ON THE PROPOSED DESIGN

The availability of $p\bar{p}$ collisions at 540 GeV c.m. energy will permit studies of much shorter range interactions than at existing machines, usually leading to large transverse momentum secondaries. Among such interactions the possible production of $W^{\pm}$ and Z^0 weak bosons is of prime importance. Also, the short-distance structure of hadrons is likely to manifest itself by the production of large transverse momentum hadron jets. The proposed apparatus aims at investigating these two phenomena in the simplest possible way.

With a nominal luminosity of 10^{30} cm^{-2} s^{-1} the rate of $W^{\pm}$, Z^0 production expected from current quark fusion models does not exceed a few hundred per year. The necessity to cover a large fraction of the solid angle is therefore imposed upon us.

The large transverse momentum electrons from $Z^0 \rightarrow e^+ e^-$ and $W^{\pm} \rightarrow e^{\pm} \nu$ decays provide an excellent signature because calorimetric techniques permit the measurement of 50 GeV electron energies to an accuracy of a few percent. The momentum measurement of electrons to the same accuracy would require a large volume of high magnetic field around the beam interaction region.

Electron identification in the presence of a large hadronic background is of crucial importance. In this energy domain, the only simple technique is that of shower counters ; rejection against charged hadrons results from the fact that they usually do not deposit a large fraction of their energy in the shower counter. To obtain a significant improvement of this rejection power with momentum measurement requires an accuracy as good as that of the energy measurement. This is difficult to achieve at 50 GeV/c. The presence of a magnetic field would help to solve the "overlap" problem (a high transverse momentum π^0 accompanied by a soft charged hadron in its neighbourhood) but would make it difficult to reject electrons from π^0 Dalitz decays. In the proposed experiment the "overlap" background is not expected to exceed one percent of the inclusive π^0 yield (see Section 2.3).

The above considerations led us to the choice of a detector having no magnetic field in the central region.

A specific feature of the $\bar{p}p$ collider is the charge asymmetry of the W-decay electrons. It is expected to be large and opposite to that resulting from strong interaction backgrounds. Because of the unique signature of the weak interaction provided by this effect we have decided to devote effort to its observation. This implies the necessity of charge measurement in the angular region between 20^0 and 40^0, where this asymmetry is expected to be large. To this end we propose to use two magnetic spectrometers (toroidal fields) followed by segmented shower counter arrays (see Section 3).

In order to observe the hadronic decays of the Z^0 and $W^{\pm}$ bosons (which are expected to occur with a large branching ratio) and in order to study large transverse momentum hadron production, we propose to complement our detector with hadron calorimetry in the central region. This provides an easy trigger and a good energy measurement. It also improves the identification of $W^{\pm} \rightarrow e^{\pm}\nu$ decays from the missing neutrino transverse energy, and, more generally, helps in hadron rejection (see Section 2).

A powerful vertex detector allows the measurement of very high multiplicities and the observation of collimated jets.

Furthermore we wish to study the sharing of momentum within large transverse momentum jets. This requires the momentum analysis of jet fragments. We propose to perform this measurement in a 30^0 azimuthal wedge, a technique which has been very useful at the ISR. During the initial operation of the collider, when the luminosity may not have reached its design value, it will then be possible to measure inclusive spectra of charged particles and π^0's as well as correlations among them. Owing to the simplicity of the proposed magnetic spectrometers and the consequent ease of data analysis, very early results could be obtained.

The modularity of the central detector permits its conversion to a calorimeter having full azimuthal coverage if desired at a later stage (see Section 4).

2. - BACKGROUNDS IN THE SEARCH FOR W → e ν.

2.1 - Introduction

In this section, we present a detailed discussion of the various kinds of backgrounds which could simulate W → e ν events. Since most of these backgrounds result from the production of high p_T hadrons in $\bar{p}p$ collisions, we have studied these final states by means of a Monte Carlo program, in which high p_T hadrons, or jets of hadrons, are generated according to a quark-quark scattering model. Initial quark distribution functions and final quark fragmentation functions are taken from Feynman and Field [1], while the elementary quark-quark scattering cross-section is tuned to give the desired p_T-dependence of the single hadron inclusive cross-section. To be consistent with assumption B of our proposal (see Eq. 2.1.2 of SPSC/P93), we have forced the model to generate a p_T^{-4} dependence.

These Monte Carlo studies have been invaluable to understand some types of background events and have led us to make minor modifications to the proposed apparatus. In addition, they have provided quantitative estimates of the background rejection which can be obtained by the requirement that the electron transverse momentum appears unbalanced in final states containing a W → e ν decay, whereas background electrons are in general accompanied by a high p_T jet of hadrons at opposite azimuthal angle.

Other aspects of hadron rejection have been studied experimentally using electrons and pions up to energies of 60 GeV from the SPS. We have taken advantage of the fact that some of us (the Orsay group) are at present involved in experiment WA-2, which uses the Y-1 beam in the West Area. This beam can be converted into an electron-enriched beam by placing a lead plate 1 metre downstream of the production target and retuning the beam optics. These studies are described in detail in Appendix 1.

It is probably worthwhile to recall that most of the authors of the present proposal have been involved, during the last few years, in experiments whose main goal was the detection of direct electrons in the presence of a hadronic background. These experiments have been, or are being, performed with different techniques, and in different electron energy

domains. At the ISR, experiments R-102, R-105 and R-702 used a magnetic spectrometer, gas Cerenkov counters, shower detectors and no magnetic field on the interaction volume. Experiment R-103 used no magnetic field at all, but just shower detectors. The present experiment R-108, on the other hand, uses a solenoid magnetic field on the interaction volume, and shower detectors. In a different energy domain, experiment WA-2 uses a magnetic spectrometer together with transition radiation and shower detectors. Furthermore, two of us (J.-M. G. and J.-P. R.) were involved in experiment E-70 at Fermilab, which observed the production of direct electrons using a magnetic spectrometer and shower detectors.

On the basis of this collective experience, we are aware of the advantages and disadvantages of the various techniques which could be used to detect high p_T electrons from $W \to e \, \nu$ decay at the $\bar{p}p$ collider. In particular, we are convinced that the best technique to reject hadron backgrounds is represented by a combination of a magnetic spectrometer and a shower detector with comparable momentum and energy resolution, with the addition of gas Cerenkov counters or transition radiation detectors and no magnetic field on the interaction volume. However, it is very difficult to design such an apparatus with a solid angle large enough to make it useful for a search of the decay $W \to e \, \nu$, given the low event rate expected at the $\bar{p}p$ collider. For this reason we have adopted the proposed solution which in our opinion has the advantage of large solid angle coverage together with the necessary hadron rejection to detect the decay $W \to e \, \nu$ above the expected backgrounds.

2.2 - Background from photon conversion and Dalitz decays.

The production of high p_T π^0 or η mesons may give rise to high p_T electrons either by their normal decay into two photons, one of which undergoes conversion in the SPS vacuum chamber, or by Dalitz decay. Assuming a ratio $\eta/\pi^0 = 0.5$ at production, the yield of electrons from these two mechanisms together amounts to 3.5% of the single π^0 yield at the same value of p_T, assuming a steel vacuum chamber with an average thickness of 0.2 mm. In most of these events, the opening angle of the e^+e^- pair is so small that the two particles appear as a single track in the detector. This configuration is easily identified by measuring the

pulse height of the scintillation counter traversed by the two particles in the vertex detector. The requirement that the pulse height corresponds to that of a single minimum ionising particle reduces this background by a factor $\sim$ 10. It must be pointed out that for Dalitz decays this method yields a worse rejection if a magnetic field is present over the $\bar{p}p$ interaction volume. In this case the magnetic field separates the two particles, which then cross in most cases two different counters. This is especially true because of the generally asymmetric energy sharing between e^+ and e^- in a Dalitz decay.

In the regions of the apparatus where the vertex detector is followed by a magnetic field, the rejection of this type of background is higher than the value quoted above. The presence of an additional photon in the final state results in fact in a measurable difference between the momentum and the shower energy.

In summary, we estimate that electrons from photon conversions and Dalitz decays contribute at most 3.5×10^{-3} of the single π^0 yield to the single electron signal.

2.3 - Overlap background.

This is probably the most serious source of background in an apparatus which does not use a magnetic field. It results from a high p_T π^0 or η meson which produces an electromagnetic shower, accompanied by one, and only one, charged particle of any momentum within the angular resolution of the shower detector. In our original proposal, this resolution is defined by the size of a calorimeter cell which subtends 10° in θ and 15° in azimuth in the central detector.

We have estimated the contribution of this type of background by means of the Monte Carlo program described in Section 2.1. The amount of overlap background expected in the framework of this model depends on the transverse momentum of the hadrons in a jet with respect to the jet axis. We have assumed a distribution of the type $k_T e^{-b\,k_T^2}$, with $\langle k_T \rangle = 0.5 \sqrt{\pi/b} = 0.6$ GeV/c. Larger values of $\langle k_T \rangle$ would result in smaller contributions from the overlap background.

Under these assumptions, and for an angular resolution of $\pm 5^\circ$ in the measurement of the neutral meson direction, we find that the overlap

background contribution to the single electron signal is $\sim$ 25% of the single π^0 yield in the p_T interval between 20 and 70 GeV/c. This high value is a consequence of the large momenta involved, which result in a stronger jet collimation than found, for example, in experiments at smaller smaller p_T values.

In order to improve the angular resolution in the measurement of the electromagnetic shower, we intend to add to the vertex detector another MWPC located just in front of the central calorimeter, at an average distance of 40 cm from the collision point. This chamber is preceded by a lead thickness of 2 or 3 radiation lengths. Its cathode planes consist of helical strips, equipped with pulse height measuring electronics. The purpose of this chamber is to detect the shower initiated in the lead by the photons from π^0 or η decay, and to measure the centroid of the shower as a way to determine the space position of the photons. The conversion probability in lead is 0.79 (0.90) for a thickness of 2(3) radiation lengths and for each photon.

We have experimentally investigated the feasibility of this method using electrons of 15, 28 and 50 GeV from the Y-1 beam (see Appendix 1). The conclusion of these tests is that it is possible to localise the shower with an accuracy of better than $\pm$ 1.0 cm. This corresponds to an angular resolution of $\pm$ 1.0/40 = $\pm$ 25 mr, instead of $\pm$ 90 mr in θ and $\pm$ 135 mr in ϕ as given by the size of a calorimeter cell.

With this improved resolution, the overlap background decreases to the level of 10% of the single π^0 yield. However, a further rejection factor is available from the fact that if a charged hadron overlaps the high p_T neutral meson within the angular resolution given above, its momentum is predicted by the model to be rather high. This is illustrated in Fig. 1a, which shows the momentum distribution of the charged hadrons accompanying a π^0 of p_T > 20 GeV/c within a cone of 25 mr half aperture. This distribution is characterised by a broad peak at 10 GeV/c and an average momentum of 19.5 GeV/c. About 92% of the hadrons have a momentum larger than 5 GeV/c. In the proposed apparatus, overlap events will in general appear as a shower in the lead compartment of a calorimeter cell, with another shower in the iron compartment just behind, corresponding to an energy deposition too high to be explained as the leakage of the

electromagnetic shower. Hence a large fraction of the overlap events will be rejected by the requirement that the energy deposited in the iron compartment of a calorimeter cell does not exceed a given, small fraction of the energy deposited in the lead compartment.

This rejection factor will be measured experimentally by exposing a prototype calorimeter cell, at present under construction, to a high energy beam of electrons and pions. However, awaiting the results of these tests, we have tried to estimate it by means of a Monte Carlo calculation which follows the development of hadronic and electromagnetic showers throughout the structure of a calorimeter cell. For the electromagnetic shower, we use a home-made program, whose results agree with those of published programs [2]; for the hadronic showers, we use the program written by A. Grant [3].

In the calculation, we assume that a π^0, with energy $E(\pi^0) = 50$ GeV, overlaps in space with a charged π of energy $E(\pi)$, and require that the energy deposition in the iron compartment does not exceed 4 GeV, a value corresponding to 90% efficiency for the π^0. The rejection factor corresponding to this requirement increases with $E(\pi)$ as shown in Fig. 1b. If we weight each momentum bin by the distribution of Fig. 1a, we obtain an average hadron rejection factor of ~ 12. This brings the contribution of the overlap background to the single electron signal down to a level corresponding to 8×10^{-3} of the single π^0 yield.

It must be pointed out that the jet structure of high p_T hadronic events, although being responsible for the overlap background, offers other means to reject the background itself. As an example, we have estimated, in the framework of the model discussed in Section 2.1, the average number of charged particles accompanying a high p_T hadron within a given solid angle, and we have compared it to the number expected in the same solid angle around an electron from the decay $W \rightarrow e \ \nu$. The latter has been calculated assuming that the hadrons produced together with the W have p_T and y-distributions which are similar to those of a normal event with an effective total centre-of-mass energy $\sqrt{s}_{eff}$ given by :

$$\sqrt{s}_{eff} = \{ \ (\sqrt{s} - E_W)^2 - p_W^2 \ \}^{\frac{1}{2}} \ ,$$

with $\sqrt{s} = 540$ GeV. In addition, we take into account the centre-of-mass

motion of this system, which recoils against the W.

We find that in a solid angle defined by a cone of 10° half-aperture around the high p_T particle, only 3.5 x 10^{-3} of the electrons from $W \to e\ \nu$ are accompanied by another charged particle, whereas this is the case for 91% of the hadronic events. Hence the requirement that no other charged particle is present in such a cone around the electron track would further reduce the hadronic background by a factor of 11, with a negligible effect on the $W \to e\ \nu$ detection efficiency. It should be pointed out that, if the jets are more collimated than assumed above, the overlap background increases but this rejection factor increases also.

Finally, we discuss the overlap background in the two regions covered by the toroidal magnets. The size of each segment of the shower detector used in this region, corresponds to an angular resolution for photons which is very similar to that of a calorimeter cell in the central detector. Using the Monte Carlo calculation described in Section 2.1, we find that 20% of the π^0's with $p_T > 20$ GeV/c detected in the shower counter are accompanied by a charged particle within the angular resolution of a segment. However, we measure the momentum of this charged particle with a resolution $\Delta p/p = 0.005\ p$, where p is the momentum in GeV/c. It is then possible to compare the measured value of p to the shower energy E, and to reject the background by a suitable cut on the variable $(p-E)/E$. We find that only 14% of the overlap events satisfy a cut which corresponds to 90% efficiency for the electrons. We expect, therefore, the overlap background to contribute 2.8% of the single π^0 yield in the backward-forward spectrometers.

2.4 - Background from high p_T charged hadrons.

This type of background results from a single charged hadron which deposits most of its energy in the electromagnetic shower detector and thus simulates an electron.

In the central detector, we have two criteria to reduce this type of background. The first is a suitable cut on the pulse height recorded in the MWPC located after the lead thickness, to require that the shower has been initiated in the lead. This method uses the well-known fact that electrons are characterised by an early shower development, whereas hadrons in general do not show this feature. It is known that good hadron rejections

can be achieved in this way [4].

The second criterion is a suitable cut on the ratio between the energy deposited by the particle in the lead compartment of a calorimeter cell, and the total energy deposited in the whole cell. The latter quantity is a measure of the total particle energy. In the case of a genuine electron, this ratio is very close to 1, whereas it is in general smaller than 1 for charged hadrons.

In the regions of the detector where a magnetic field is present, the particle momentum is directly measured, of course.

In the shower counters located after the toroidal magnets, the method of the early shower development can be used thanks to the sampling of the shower after 2 and 7 radiation lengths, as described in Section 3.

We have measured the rejection factor which can be obtained by these methods, using pions of 55 and 60 GeV from the Y-1 beam (see Appendix 1). We find that an overall rejection factor of at least 200 against hadrons can be obtained with a combination of cuts which corresponds to 90% electron efficiency (see Appendix 1). We conclude, therefore, that the single charged hadron background will contribute to the single electron signal at a level of less than 5×10^{-3} of the single hadron yield.

2.5 - Background rejection by p_T balance.

If the W boson is produced with small transverse momentum $(p_T(W) \ll M_W/2)$, most of the transverse momentum of the electron from the decay $W \to e \, \nu$ is then balanced by the neutrino. Events containing a $W \to e \, \nu$ decay will be characterised, therefore, by an apparent imbalance of the electron p_T. On the other hand, in the case of background electrons no neutrino is involved and the electron p_T is balanced by hadrons, or jets of hadrons, at opposite azimuthal angle. This is a dramatic difference, which can be used to achieve a further rejection against background.

It is not clear at present what will be the W transverse momentum at $\sqrt{s} = 540$ GeV. Recently several theoretical papers [5] using QCD have suggested that the average p_T value of systems resulting from $\bar{q}q$ fusion may increase with increasing $\sqrt{s}$ for fixed $\bar{q}q$ mass. For the case of W production, $\langle p_T \rangle$ values as high as 10 to 20 GeV/c have been predicted.

Results on $\mu^+\mu^-$ production from p-nucleon collisions at Fermilab

(Experiment E-288), though being consistent with these theoretical ideas, are inconclusive, due to the rather small interval of $\sqrt{s}$ (19 to 27 GeV) which is covered in that experiment.

Independently of these arguments, we have estimated the background rejection which can be achieved in the proposed apparatus by this method, under the assumption that $p_T(W)$ is small. In this study, we have used the Monte Carlo program described in Section 2.1 to generate jets of hadrons at high p_T. If a hadron in one of the two jets has a transverse momentum above 20 GeV/c, we assume that it simulates a single electron with the same value of the transverse momentum p_T^e. We then look at the other jet, and add up the momenta of all the particles (assumed to be pions) which hit the sensitive part of the apparatus. We then define a total transverse momentum P_T which is compared to the value of p_T^e by forming the ratio $R = P_T/p_T^e$. This ratio represents the fraction of p_T^e which is balanced by detected particles. As mentioned before, unless the W is produced with large p_T, very small values of R are expected for events containing $W \rightarrow e \, \nu$ decays.

Under the assumption made in our proposal, namely that $<p_T(W)> = 1.5$ GeV/c, it is reasonable to accept as $W \rightarrow e \, \nu$ candidates all of the events for which $R < 0.2$. For a mass of the W of 70 GeV, p_T^e is peaked at 35 GeV/c (see Fig. 17 of SPSC/P93), and values of R smaller than 0.2 correspond to events in which less than 7 GeV/c of total transverse momentum are detected at opposite azimuthal angles. This happens for practically all $W \rightarrow e \, \nu$ decays, hence the cut $R < 0.2$ does not affect the $W \rightarrow e \, \nu$ detection efficiency.

For the central detector, we find that the rejection factor achieved against background events by the cut $R < 0.2$ depends on p_T^e, decreasing from 32 at $p_T^e = 25$ GeV/c to 13 at $p_T^e = 55$ GeV/c. At $p_T^e = 35$ GeV/c, this factor is 22.

We find further that a large fraction of the background events satisfy the cut $R < 0.2$ because the hadron jet at opposite azimuth angle is pointing towards one of the two 15° wide obstructions represented by the coils and pole pieces of the large angle magnetic spectrometer (LAMS). If we remove the LAMS and complete the central detector over the full azimuth with calorimeter cells, the rejection factor due to the $R < 0.2$ cut now becomes an increasing function of p_T^e, varying from 100 at $p_T^e = 25$ GeV/c to 227 at

p_T^e = 55 GeV/c. This different behaviour is due to the fact that in the presence of an obstruction, more particles are lost at higher momenta because of the higher jet collimation.

However, in view of the strong azimuthal correlation of the two jets, which are essentially back-to-back in azimuth, rejection factors as good as the ones just quoted are also available with the LAMS present, if one excludes two azimuthal regions approximately 20° wide, centred at azimuth angles opposite to those of the LAMS coils. More generally, we can say that the LAMS coils, as well as the toroid coils, produce a modulation of the rejection factor with the azimuth angle ϕ. We note that the central detector can be easily modified by replacing the LAMS with four additional azimuthal arrays of calorimeter cells, should the need for this modification be compelling.

We would also like to point out that, for the case in which the balancing jet goes into the regions covered by the toroidal magnets, we are able to measure the energy of photons and the momentum of charged particles only. Due to the absence of a hadronic calorimeter in these regions, particles like neutrons and K_L^0's are lost. We do not know how to estimate the effect of these particles. However, we find that, even if the two forward spectrometers did not exist at all, the rejection factor from the central detector alone would still be of the order of 10.

Finally, we find that the cut R < 0.2 applied to events in which the electrons are detected in the two forward spectrometers provides a background rejection factor of 24 at p_T^e = 35 GeV/c. Again, this factor becomes much larger ($\sim$ 140) if the electrons detected at azimuth angles opposite to those of the LAMS and toroid coils are excluded.

2.6 - Conclusions.

We have made studies, using both Monte Carlo programs and measurements with electron and pion beams of energies up to 60 GeV, of the hadron rejection which can be achieved with the proposed apparatus. We find the following contributions of the various backgrounds, expressed as a fraction of the single hadron yield at high p_T :

- 3.5 x 10^{-3} from photon conversion and Dalitz decays;
- 8 x 10^{-3} from overlap background in the central detector, 3 x 10^{-2} in the two forward spectrometers;

- $< 5 \times 10^{-3}$ from single charged hadrons at high p_T.

In addition, a further average rejection factor of ~ 20 can be achieved by the requirement that at most 20% of the electron p_T value is balanced by other particles at opposite azimuthal angles. This factor applies equally to all of the three types of backgrounds mentioned above.

It appears also possible to achieve an even larger rejection by counting the number of charged particles in a small solid angle centred around the electron direction. This factor, which is of the order of 10, results from the expected jet structure of hadronic final states at high p_T.

We note that all of the rejection factors discussed above, with the exception of that resulting from the p_T balance, apply independently to each electron of a high mass e^+e^- pair, as in particular the decay $Z^0 \rightarrow e^+e^-$.

REFERENCES

1) R.D. Field and R.P. Feynman, Phys. Rev. $\underline{D15}$, 2590 (1977).

2) E. Longo and I. Sestili, Nucl. Instr. Methods $\underline{128}$, 283 (1975).

3) A. Grant, unpublished.

4) T. Massam et al., Nuovo Cim. $\underline{39}$, 464 (1965).

5) K. Kajantie and R. Raitio, U. of Helsinki report HU-TFT-77-21 (1977);

    H. Fritzsch and P. Minkowski, CERN-TH-2400 (1977);

    H.D. Politzer, Harvard report HUTP-77/A029;

    T.M. Yan, Cornell report CLNS 369 (1977);

    I. Hinchliffe and C.H. Llewellyn-Smith, Oxford report 100/76 (1976);

    P. Kreiss and K. Schilcher, U. of Mainz report MZ-TH 77/8 (1977);

    R.C. Hwa, S. Matsuda and R.G. Roberts, RHEL report RL-77-117/A
    T 207 (1977);

    F. Halzen and D.M. Scott, Wisconsin report COO-881-16 (1978);

    K. Kinoshita, et al., Physics Letters $\underline{68B}$, 355 (1977);

    D.E. Soper, P.R.L. $\underline{38}$, 461 (1977);

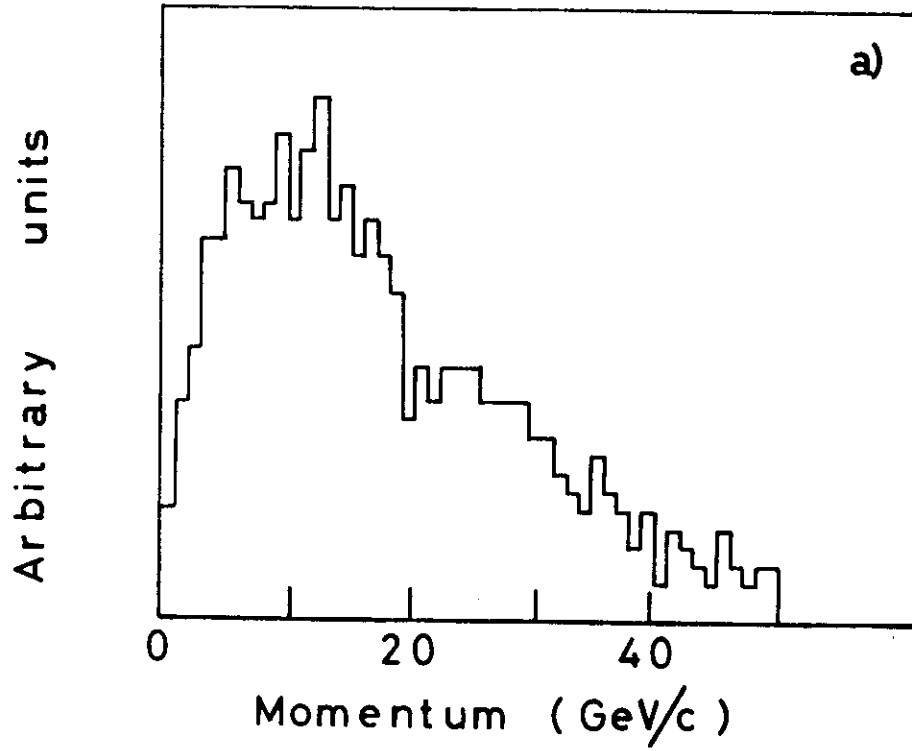   P.V. Landshoff, Cambridge report DAMTP 76/23 (1976).

Fig. 1a – Momentum distribution of the charged hadrons accompanying a π^0 of $p_T > 20$ GeV/c within a cone of 25 mr half aperture.
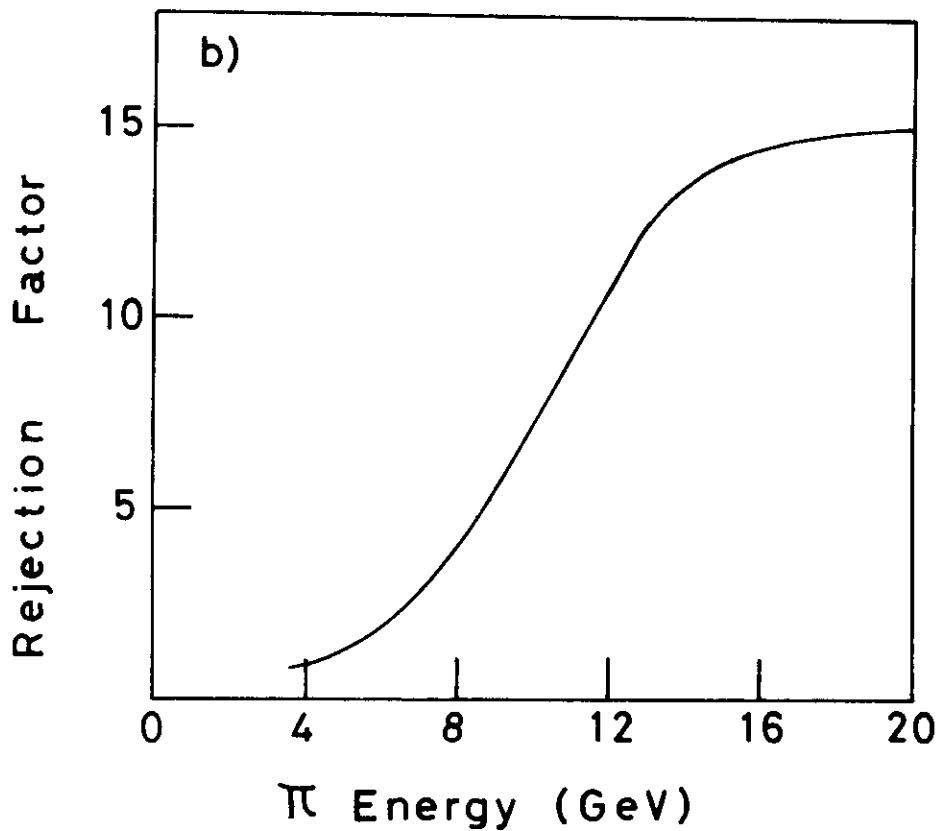

Fig. 1b – Hadron rejection factor from calorimeter cuts (see page 8).

3 - FORWARD AND BACKWARD DETECTORS

The design of the forward/backward detectors is shown in drawing 1 appended to Section 4. The chamber system is composed of 6 drift planes grouped in pairs. The frames of these chambers are in the shadow of the toroid coils. The wires of three planes are parallel to the magnetic field in the middle of the corresponding sector. The wires of the other three chambers are tilted by 10^0 in order to be able to reconstruct tracks in space. Right-left ambiguities are solved by using wire doublets. The lever arm for direction measurement is 80 cm and a precision of 200 μm is expected. Very high momentum particles will be almost perpendicular to these chambers and therefore the 200 μm precision can easily be achieved with a drift space of 2.5 cm. The complete chamber system is mounted on a rotating wheel to facilitate chamber replacement. We have increased the number of drift planes from 4 to 6 to improve pattern recognition. The origin of the particle is taken to be the interaction vertex as measured from the tracks in the vertex detector.

The lead glass array of the original proposal is replaced by a 25 rl thick sandwich of lead-scintillator (0.5 rl of lead interspaced with 5 mm of scintillator) which is less sensitive to radiation damage. In each toroidal sector the shower counter is segmented in 10 parts. Each array is then composed of 120 elementary cells, each covering an angular interval $\Delta\theta = 4^0$ and $\Delta\phi = 12^0$. Assuming a flat rapidity distribution, the particle flux in a cell is similar to that in a central calorimeter cell. Light collection is achieved by wavelength-shifting light guides of 5 mm thickness (BBQ). It is planned to collect separately the light over the first 2 rl and over the following 5 rl in order to improve the hadron rejection. Above 10 GeV/c, a rejection better than 200 can be expected against hadrons.

The shower counter system is mounted on a rigid frame. Two elementary cells in a sector at the same radius are grouped in one mechanical device, which is a box with a 2 cm thick iron plate at the front supporting the two elementary cells and 0.15 cm iron side walls. For each elementary cell four rods (1.4 cm diameter) are fixed perpendicular to the front plate. Four holes are drilled in the lead and scintillator plates in

order to stack them along the rods. The stack is then bound rigidly together, and all the stresses are taken by the front plates. Notches on the sides of the front plates prevent the cells from sliding with respect to each other. The BBQ light collectors are placed on three sides of each calorimeter cell. The cells weigh between 125 and 200 kg each. The support structure is in the shadow of the toroid coils. Each cell sits in a sliding rack. The total weight of each detector is 19 tons. The 2 cm thick iron plate also shields the phototubes from the stray magnetic field of the toroid.

4 - DETECTOR DESIGN : MECHANICAL ASPECTS

The present section provides clarifications on the mechanical aspects of the detector design, a topic which had not been discussed in detail in proposal P93. We shall mainly concentrate on features which are either unconventional or specific to operation in the SPS tunnel. We have assumed that the design of the experimental area corresponds to the preliminary study recently made by the SPS Division (Projet d'aménagement zone LSS4, SPS p̄p, Guinand, 20-04-78).

The detector consists of four independent parts which can be moved separately and parked in the assembly area. They are :

i) the central calorimeter and vertex detector,

ii) the large angle magnetic spectrometer,

iii) the forward and backward detectors (two independent units).

Drawings 1 to 4 show different views of the set-up (excluding the detectors of the large angle spectrometer, which are of a conventional design). The forward and backward detectors have been described in the preceding section. We shall therefore limit our discussion to the central calorimeter and vertex detector.

The central calorimeter is made of 20 azimuthal sectors supported by two large rings. A sector contains 10 calorimeter cells and weighs about 4 tons, including scintillators and phototubes. Each sector is separately assembled and calibrated at surface level before being transported to the SPS tunnel.

The vertex detector, a set of cylindrical chambers, is supported from the calorimeter itself. For repairs, it can be slid out of the calorimeter along the vacuum pipe.

4.1 - Design of a calorimeter sector

The sampling iron plates are screwed between two large side plates.

Machining of the sampling plates and accurate drilling of the thin ($\leqslant 5$ mm) side plates can be performed to the desired accuracy without special difficulty. Stresses in the iron side plates have been evaluated and the deformation of the structure under its own weight is negligible.

The side plates start from the inner radius of the hadron calorimeter. The lead-scintillator sandwiches of the e-m calorimeter are

embedded in thin walled boxes attached to the first sampling plate of the
corresponding cell of the hadron calorimeter. This permits a very small
wall thickness (≤2mm) between neighbouring cells.

The side plates extend beyond the outer iron sampling plates to
provide a support for the phototubes. The structure is kept rigid with
spacers inserted between the two side plates of a same calorimeter sector ;
the end spacers are used to support the whole sector.

Details of the sampling strategy (plate thickness, number of plates
and of independent read-outs, etc...) will be decided after completion
of measurements in a test beam. To this end we are constructing two proto-
type cells and have purchased scintillator, plexipop and BBQ sheets which
will be assembled in early June 1978.

4.2 - Design of the large angle magnet

In the present design a gap corresponding to four calorimeter sectors
is used for magnetic analysis. The modularity of the design allows for
conversion to a 24 sector calorimeter with full azimuthal coverage if
desired at a later stage.

The magnet coils follow the boundary of the iron cross section of the
calorimeter and provide a field integral of approximately 1 Tm.

The magnetic field induced on the beams is of the order of 200 Gauss
which can be easily compensated.

Strong forces act on the coils which must be kept apart by means of
side walls and/or pillars. Details of this structure are presently under
study but will somewhat limit the spectrometer aperture at smaller angles.

4.3 - Design of the vertex detector

The vertex detector is supported by a stainless steel cylinder
attached to the side plates of the calorimeter sectors.

A two radiation lengths thick lead converter, surrounded by a
cylindrical chamber, is installed around the support cylinder to improve
on electron identification (see Section 2). This outer structure is only
80 cm long and covers the entrance face of the central calorimeter.
A window is opened in the support cylinder and lead converter,
to match the aperture of the large angle spectrometer.

The vertex detector itself is a set of coaxial cylindrical chambers
located inside the support cylinder and surrounding the vacuum pipe. Its

inner diameter (17.2 cm) is sufficient to insert heat insulators around
the vacuum pipe during bake-outs. The chambers are grouped in three sets,
each with a length matching the angular coverage of the forward and
backward detectors. In this small angle region the support cylinder is
limited to 12 thin rods in the shadow of the toroid coils and does not
obstruct particles entering the forward and backward detectors. Tests
are underway to make the chamber walls out of carbon fiber reinforced
resin. This solution would make the chambers both light and self-supporting.

Access to the vertex detector is obtained by recessing one of the
forward/backward detectors. In addition the whole vertex detector assembly
can be slid along the vacuum pipe and through the forward/backward
detectors.

4.4 - Installation

The large support rings are first put together in the assembly area.
The calorimeter sectors are installed next, one after the other. During
this operation they are handled by means of a special tool fixed on their
outer side plate. The magnet coils are installed last.

After inserting   the vertex detector and fixing it to the calori-
meter sectors, the whole assembly is ready to be rolled into the experi-
mental area.

The assembly operation will be first performed at surface level to
gain experience and to solve possible unexpected difficulties.

4.5 - Toroidal magnets

The toroidal magnets are part of the forward/backward detectors and
are supported on the same structures as both the drift chambers and the
lead-scintillator sandwiches (see Section 3).

The coil design was described in our proposal. Each coil, with its
iron core pole piece, is inserted in a thin walled frame. Rigidity
between the 12 coils of a same toroid is achieved by means of two
conical structures with openings matching the aperture of the forward/
backward detectors. The outer cone is linked to the support rings of
the central calorimeter during normal operation but can be easily
decoupled when required. The main forces acting on the toroid coils
have been evaluated. Some further model studies are necessary to finalise
the design of the support structures in the region of the large angle
magnetic spectrometer.

FIGURE CAPTIONS (Section 4)

Drawing 001-0 : Vertical cut along the beam.

002-0 : The forward detector in its recessed position.

003-0 : Transverse cuts normal to the beam.

004-0 : A view of the forward detector.

5 - MEMBERSHIP OF THE COLLABORATION

5.1 - The Collaboration has been enlarged to include a group from Pavia (University and INFN).

5.2 - The Saclay group, the Pavia group and half of the CERN group have recently been running ISR experiments and have now completed data taking. Data analysis is well advanced (and almost completed for what concerns the Pavia group). These groups have no other committment and can already devote a major fraction of their time to the preparation of the proposed experiment. By the end of 1978 they will be in a position to devote the totality of their effort to it.

5.3 - The Orsay group and the other half of the CERN group are presently running experiments at the SPS (WA2) and at the ISR (R 108). In both cases data taking should be completed by the end of the year. These groups are already in a position to devote a fraction of their time and effort to the proposed experiment. This is well suited to our needs during the preparation of this experiment. Their committment to the proposed experiment should reach 100 % by the end of 1979.

5.4 - All four groups have strong technical support at their home laboratories.

APPENDIX 1

EXPERIMENTAL STUDY OF THE EARLY DEVELOPMENT OF ELECTRON AND HADRON SHOWERS

This appendix describes a measurement performed in the Y_1^- beam of the SPS to estimate the hadron rejection of the detector of proposal P 93.

1. APPARATUS

We have taken the opportunity offered by the present running of the hyperon experiment WA2 to perform this test using only 2.5 hours of beam time. The hyperon beam can be tuned into a rather clean electron beam, by converting photons from π^0's at the entrance of the magnetic channel. The electron momentum can be varied from 2 to more than 60 GeV/c.

At the exit of the channel the particles are bent vertically by ± 4 mrad in a first small magnet M_1, then horizontally in the spectrometer magnet M_2 by 10 mrad (Fig. A1). The particle directions are measured on each side of the two magnets, and its momentum is thus determined with a relative accuracy of ± 3% with M_1 and ± 1.3% with M_2.

In this test we have used four electron detectors (Fig. A1) :
- a first transition radiation detector located upstream of M_2. It consists of a lithium radiator followed by a xenon-CO_2 proportional chamber and is used to improve off-line the purity of both the electron and the hadron beams by a factor ~ 10.
- a xenon-CO_2 wire chamber working in the proportional mode, located downstream of M_2. This chamber is normally used as part of a second transition radiation detector. The pulse heights of the wire signals are measured in ADC's. For the first part of this test two lead plates were inserted in front of the chamber, one 11 mm thick (2rl) facing the lower half, the other 16 mm thick (3rl) facing the upper half (Fig. A1). This arrangement measures the charge multiplicity of showers originating in the lead.
- a large multiwire proportional chamber located 10 meters downstream of M_2 (the photon chamber). It is preceded by a 2rl thick lead plate and

is normally used to detect photons. It has been used as a second independent measurement of the shower development. Since the wires are not connected to ADC's but only to threshold amplifiers, a variable sensitivity was achieved by reducing the operating voltage.

- a lead glass array, located behind and against the photon chamber. It is 18rl thick and is split into 3 identical layers. In this test it is used to simulate the electromagnetic compartment of the $\bar{p}p$ central calorimeter.

2. DATA ANALYSIS AND RESULTS

Data were taken with electrons at the three energies of 15, 28 and 50 GeV, and with pions at 55 and 60 GeV.

2.1 Lateral shower size

From the first test performed with the $Xe-CO_2$ chamber we have a direct measurement of the charge multiplicity in the shower after 2 and 3 rl, once the chamber gain is calibrated. Multiplicity spectra are shown in Fig. A2 for 28 and 50 GeV electrons, for 55 GeV pions after 2 rl and for pions not traversing the lead. It is clear that the multiplicity measurement already gives a good separation between electrons and hadrons.

Due to the 10 cm distance from the lead to the chamber, which we could not avoid in this test, and also due to the fringe field of M_2, the lateral shower size is increased. Nevertheless, we can localise the shower with an accuracy of ± 10 mm as shown in Fig. A3a for 28 GeV electrons and in Fig. A3b for 55 GeV pions. These distributions are obtained by calculating the mean position of the wires weighted by the corresponding pulse heights. With 50 GeV electrons the accuracy becomes ± 7 mm.

In the second part of the test which uses the photon chamber, we can also determine the shower position after 2 rl of lead from the mean position of the wires hit. This is shown in Fig. A4 for 50 GeV electrons and in Fig. A5 for 55 GeV pions at four operating voltages, reduced in steps of 100 volts from the nominal operating value.

Here again we observe that even at the lowest voltage the chamber remains fully efficient for electrons while its efficiency for pions drops to 5%. We find that the localisation of electrons improves at lower voltage and compares well with the results of the first test.

Both tests show that the electron shower can be localised with an accuracy of ± 10 mm. This accuracy would be even better using a chamber which would combine a pulse height measurement and a shorter distance to the lead plate.

2.2 Hadron rejection

From the results shown in Fig.A2 we see that a minimum requirement of 4 charged particles does not lose electrons, and does reject pions efficiently. Equivalently, from Fig. A4 and A5 we see that a decrease by a factor of 8 (corresponding to the ~ 300 volt point) in the gain of the photon chamber leads to the same result.

The primary rejection against hadrons will be obtained in the $\bar{p}p$ experiment by requiring an electron-like energy distribution in the electromagnetic and hadronic compartments of the calorimeter. Both of the two criteria, multiplicity after 2rl and electron-like energy sampling, tend to retain hadrons which interact very early. Thus the two requirements are not independent, and their combined rejection is not the product of the individual ones.

In this test we measure the combined rejection using the data taken with 60 GeV pions. The multiplicity cut after 2rl is obtained from the photon chamber by looking for a hit within 4 cm^2 around the track at the lowest voltage used, where the chamber is still 98% efficient for electrons.

The energy sampling is obtained from the energies E_1 and E_2 deposited in lead glass layers 1 and 2 respectively. We apply the cuts $E_1/p > 0.4$ and $E_2/p < 0.55$, were p is the incident beam momentum. These cuts are 93% efficient for electron energies up to 50 GeV. In the hyperon setup there is no hadron calorimeter following the lead glass array, so one cannot directly require that the energy deposited after the electromagnetic compartment is sufficiently small. However since the hadron momentum is measured,

we can apply an equivalent condition on the quantity $(E_1+E_2)/p$. Fig. A6 shows the efficiency for 60 GeV pions as a function of the cut applied to $(E_1+E_2)/p$ under various conditions.

In conclusion the rejection resulting from the multiplicity cut is 20 when applied alone and 1.5 when applied together with the energy sampling cut. For $(E_1+E_2)/p > 0.78$, the hadron rejection is (see Fig. A6d) 430±60 for a 90% electron efficiency.

FIGURE CAPTIONS

Fig.A1   Apparatus used for the test in the Y_1 beam.

Fig.A2   Shower multiplicity distributions :
a) For 50 GeV electrons after 2 rl.
b) For 28 GeV electrons after 2 rl.
c) For 55 GeV pions after 2 rl.
d) For 55 GeV pions without lead.

FIG.A3   Shower localisation after 3 rl :
a) For 28 GeV electrons.
b) For 55 GeV pions.

Fig.A4   Shower localisation in the photon chamber at four operating voltages for 50 GeV electrons.

Fig.A5   Shower localisation in the photon chamber at four operating voltages for 55 GeV pions.

Fig.A6   Efficiency for 60 GeV pions as a function of the cutoff applied to $(E_1+E_2)/p$:
a) For all events.
b) For events with at least one particle observed in the photon chamber within $\Delta x = \pm 10$ mm and $\Delta y = \pm 10$ mm of the expected position. The chamber is run 300 volts below the nominal operating voltage.
c) For events with $E_1/p > 0.4$ and $E_2/p < 0.55$.
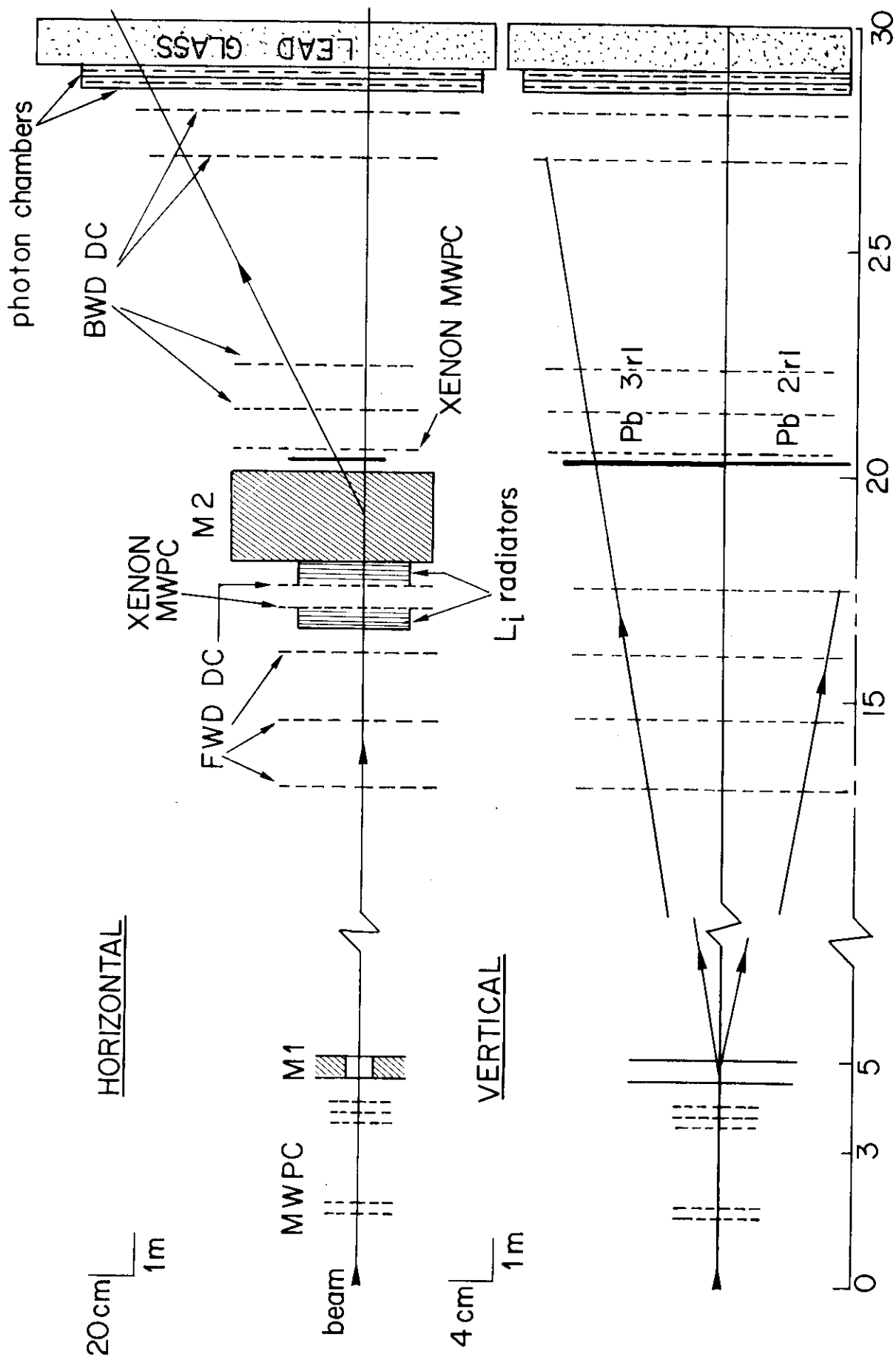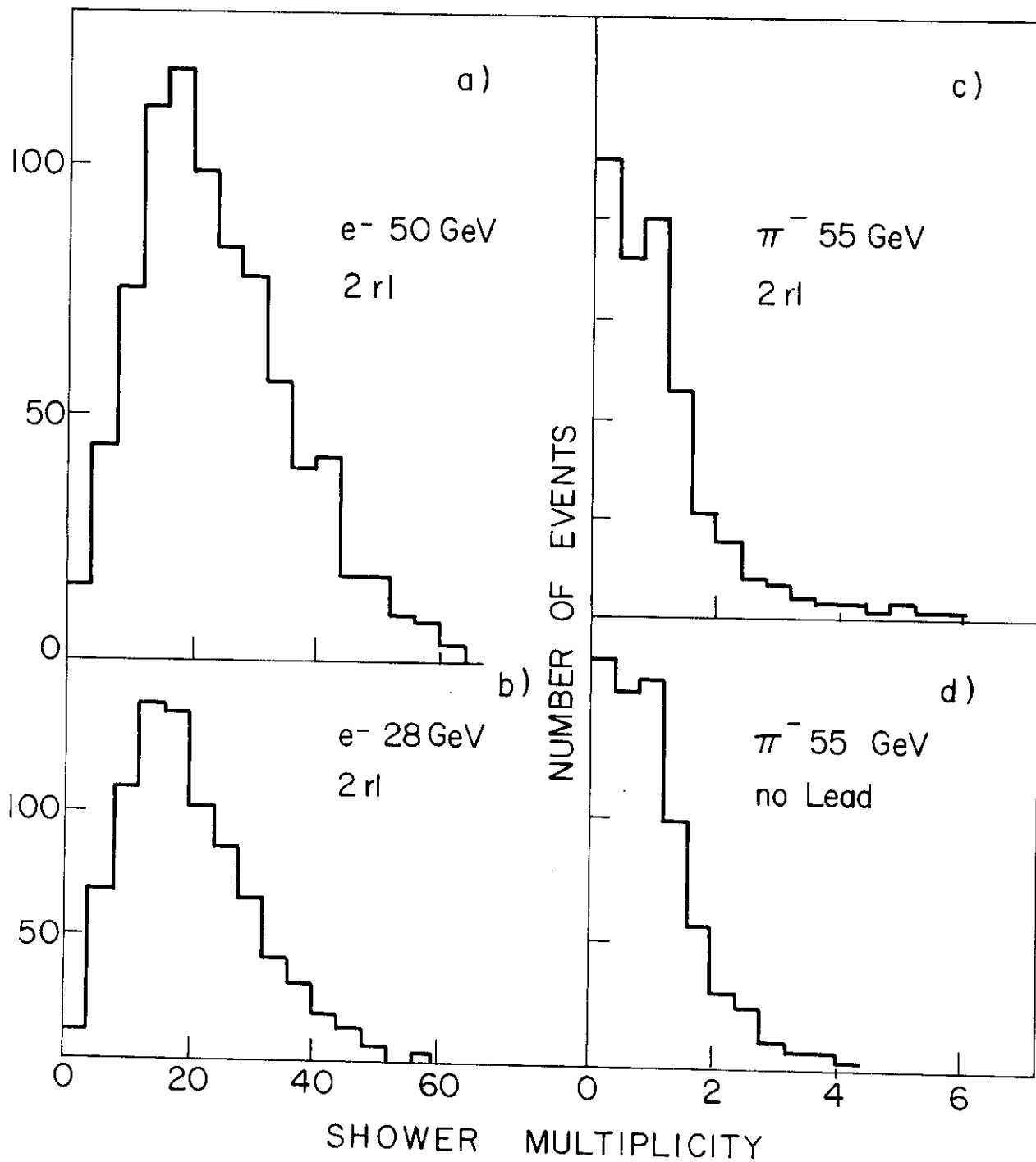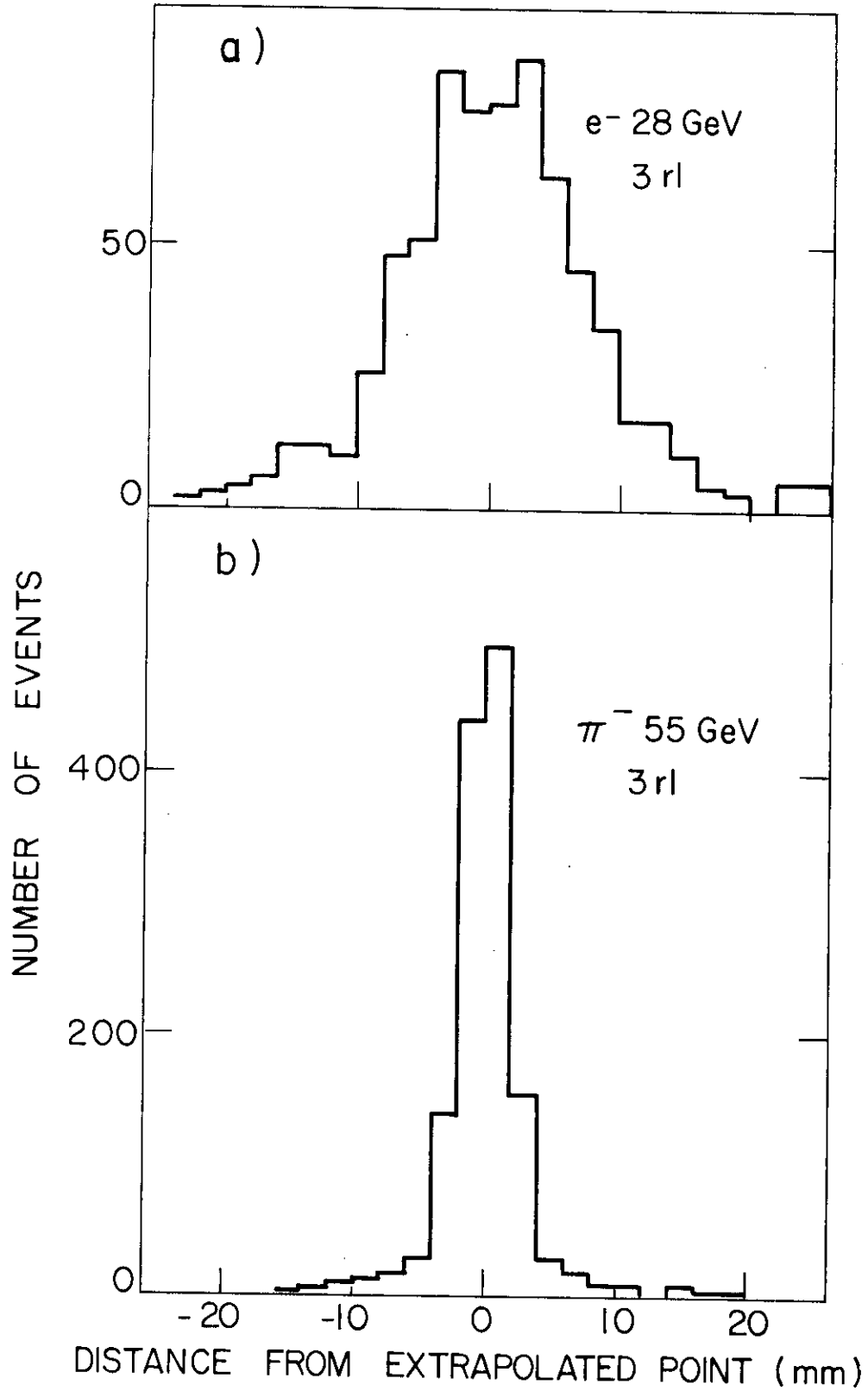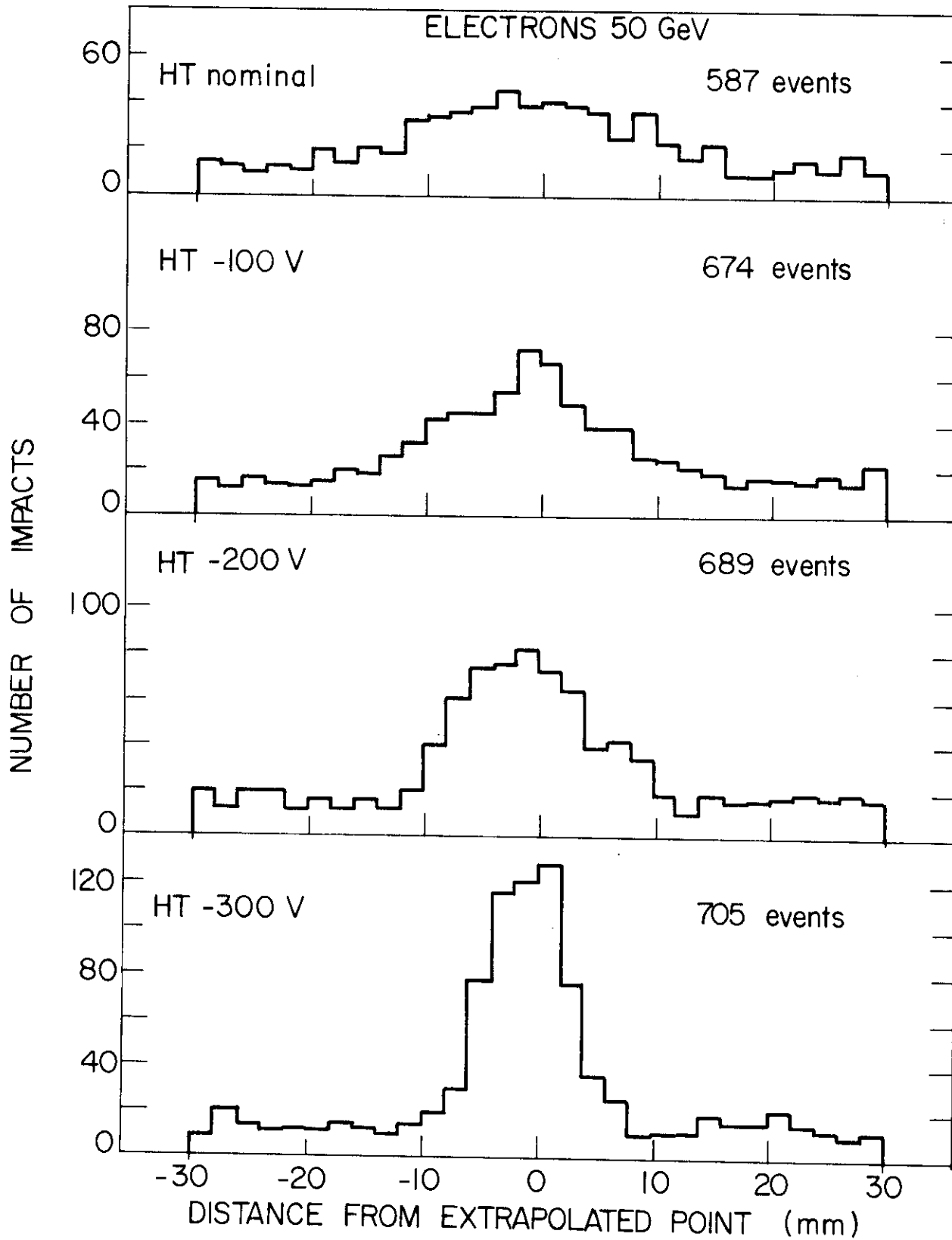d) For events which satisfy the criteria b) and c).

Fig. A1

Fig. A2

a)

e⁻ 28 GeV
3 rl

b)

π⁻ 55 GeV
3 rl

NUMBER OF EVENTS

DISTANCE FROM EXTRAPOLATED POINT (mm)

Fig. A4